PLOS ONE

RESEARCH ARTICLE

BRAPH: A graph theory software for the analysis of brain connectivity

Mite Mijalkov[1], Ehsan Kakaei[1], Joana B. Pereira[2], Eric Westman[2], Giovanni Volpe[1,3]*, for the Alzheimer's Disease Neuroimaging Initiative

1 UNAM—National Nanotechnology Research Center & Department of Physics, Bilkent University, Ankara, Turkey, **2** Department of Neurobiology, Care Sciences and Society, Karolinska Institutet, Stockholm, Sweden, **3** Department of Physics, Goteborg University, Goteborg, Sweden

* giovanni.volpe@physics.gu.se

OPEN ACCESS

Citation: Mijalkov M, Kakaei E, Pereira JB, Westman E, Volpe G, for the Alzheimer's Disease Neuroimaging Initiative (2017) BRAPH: A graph theory software for the analysis of brain connectivity. PLoS ONE 12(8): e0178798. https://doi.org/10.1371/journal.pone.0178798

Editor: Satoru Hayasaka, University of Texas at Austin, UNITED STATES

Received: February 8, 2017

Accepted: May 18, 2017

Published: August 1, 2017

Data Availability Statement: MRI Data used in preparation of this article were obtained from the Alzheimer's Disease Neuroimaging Initiative (ADNI) database (adni.loni.usc.edu) and the Parkinson's Progression Markers Initiative (PPMI) (http://www.ppmi-info.org/). Since we do not own the ADNI or PPMI data used in this study, we do not have permission to redistribute these data ourselves, as is stated in the data use agreements from ADNI (http://adni.loni.usc.edu/wp-content/uploads/how_to_apply/ADNI_Data_Use_Agreement.pdf) and PPMI (https://ida.loni.usc.edu/collaboration/

Abstract

The brain is a large-scale complex network whose workings rely on the interaction between its various regions. In the past few years, the organization of the human brain network has been studied extensively using concepts from graph theory, where the brain is represented as a set of nodes connected by edges. This representation of the brain as a connectome can be used to assess important measures that reflect its topological architecture. We have developed a freeware MatLab-based software (BRAPH–BRain Analysis using graPH theory) for connectivity analysis of brain networks derived from structural magnetic resonance imaging (MRI), functional MRI (fMRI), positron emission tomography (PET) and electroencephalogram (EEG) data. BRAPH allows building connectivity matrices, calculating global and local network measures, performing non-parametric permutations for group comparisons, assessing the modules in the network, and comparing the results to random networks. By contrast to other toolboxes, it allows performing longitudinal comparisons of the same patients across different points in time. Furthermore, even though a user-friendly interface is provided, the architecture of the program is modular (object-oriented) so that it can be easily expanded and customized. To demonstrate the abilities of BRAPH, we performed structural and functional graph theory analyses in two separate studies. In the first study, using MRI data, we assessed the differences in global and nodal network topology in healthy controls, patients with amnestic mild cognitive impairment, and patients with Alzheimer's disease. In the second study, using resting-state fMRI data, we compared healthy controls and Parkinson's patients with mild cognitive impairment.

Introduction

Graph theory studies the properties and behavior of networks, which are systems consisting of a set of elements (nodes) linked by connections or interactions (edges). Many systems found in Nature, ranging from social interactions to metabolic networks and transportation systems, can be modeled within this framework, pointing to a set of underlying similarities among these very diverse systems. The human brain can also be modeled as a network (the *human connectome*) [1], where brain regions are the *nodes* and the connections between them are the

access/appLicense.jsp). However, the data can be obtained through procedures and under conditions as described on the ADNI (http://adni.loni.usc.edu/data-samples/access-data/) and PPMI (http://www.ppmi-info.org/access-data-specimens/download-data/) websites.

Funding: Data used in the preparation of this article were obtained from the Alzheimer's Disease Neuroimaging Initiative (ADNI) and the Parkinson's Progression Markers Initiative (PPMI). Data collection and sharing of ADNI was funded by the National Institutes of Health Grant U01 AG024904 and Department of Defense award number W81XWH-12-2-0012. ADNI is funded by the National Institute on Aging, the National Institute of Biomedical Imaging and Bioengineering, and through generous contributions from the following: Alzheimer's Association; Alzheimer's Drug Discovery Foundation; BioClinica, Inc.; Biogen Idec Inc.; Bristol-Myers Squibb Company; Eisai Inc.; Elan Pharmaceuticals, Inc.; Eli Lilly and Company; F. Hoffmann-La Roche Ltd and its affiliated company Genentech, Inc.; GE Healthcare; Innogenetics, N.V.; IXICO Ltd.; Janssen Alzheimer Immunotherapy Research & Development, LLC.; Johnson & Johnson Pharmaceutical Research & Development LLC.; Medpace, Inc.; Merck & Co., Inc.; Meso Scale Diagnostics, LLC.; NeuroRx Research; Novartis Pharmaceuticals Corporation; Pfizer Inc.; Piramal Imaging; Servier; Synarc Inc.; and Takeda Pharmaceutical Company. The Canadian Institutes of Health Research is providing funds to support ADNI clinical sites in Canada. Private sector contributions are facilitated by the Foundation for the National Institutes of Health (www.fnih.org). The grantee organization is the Northern California Institute for Research and Education, and the study is coordinated by the Alzheimer's Disease Cooperative Study at the University of California, San Diego. ADNI data are disseminated by the Laboratory for Neuro Imaging at the University of California, Los Angeles. PPMI —a public-private partnership—is funded by the Michael J. Fox Foundation for Parkinson's Research and funding partners, including Abbott, Avid Radiopharmaceuticals, Biogen Idec, Bristol-Myers Squibb, Covance, Elan, GE Healthcare, Genentech, GSK-GlaxoSmithKline, Lilly, Merck, MSD-Meso Scale Discovery,Pfizer, Roche, UCB (www.ppmi-info.org/fundingpartners). For up-to-date information on the PPMI database visit www.ppmi-info.org. We would also like to thank the Swedish Foundation for Strategic Research (SSF) grant number 4-3193/2014, the Strategic Research Programme in Neuroscience at Karolinska Institutet (StratNeuro), Hjärnfonden grant number FO2015-0173, Vetenskapsrådet grant number

edges. The human brain is thus an ideal candidate for graph theoretical analysis. The nodes can be defined as the brain regions underlying electrodes or using an anatomical, functional or histological parcellation scheme. The edges are obtained as measures of association between the brain regions, such as connection probabilities (diffusion tensor imaging, DTI), inter-regional correlations in cortical thickness (magnetic resonance imaging, MRI) and electrophysiological signals (electroencephalography, EEG; magnetoencephalography, MEG) or statistical dependencies in time series (functional MRI, fMRI) and blood flow (arterial spin labeling, ASL).

After compiling all pairwise associations between the nodes into a *connectivity matrix* (or *brain graph*), several network properties can be calculated in order to characterize the global and local organization of the connectome. For instance, the *small-worldness* can be used to assess the balance between short-distance and long-distance connectivity [2], while the *modularity* defines how well the network can be divided into *subnetworks* (or *modules*) [3,4], which generally correspond to well-known brain systems such as the default-mode or fronto-parietal networks [5,6]. These network properties and many others can be used to reveal fundamental aspects of normal brain organization and highlight important aspects of underlying brain pathology in diseases such as Alzheimer's disease (AD) [7], Parkinson's disease [8], epilepsy [9,10,11], schizophrenia [12,13], multiple sclerosis [14] and autism [15].

Several toolboxes have been developed to study brain connectivity, including the Brain Connectivity Toolbox [16], eConnectome [17], GAT [18], CONN [19], BrainNet Viewer [20], GraphVar [21] and GRETNA [22]. In addition, with the emergence of time-varying brain networks as a powerful method to characterize mental illnesses [23,24], several toolboxes that allow the calculation of dynamic functional connectivity measures have also been developed [25,26]. While all of them made important contributions by proving new options to build, characterize and visualize brain network topology, they require some programming experience, or deal only with some aspects of the analysis, or are coded in such a way that their adaptation is hard to achieve. Hence, a reliable, streamlined, user-friendly, fast, and scalable software that deals with all aspects of network organization is still lacking.

In this article, we present BRAPH–BRain Analysis using graPH theory (http://www.braph.org/), a software package to perform graph theory analysis of the brain connectome. BRAPH is the first object-oriented open-source software written in MatLab for graph theoretical analysis with a graphical user interface (GUI). In contrast to previous toolboxes, BRAPH takes advantage of the object-oriented programming paradigm to provide a clear modular structure that makes it easy to maintain and modify existing code, since new objects can be added without the need for an extensive knowledge of the underlying implementation. From the clinical point of view, BRAPH presents the following strengths: (a) it allows comparing the regional mean values between groups using permutation testing to get a first impression of the data and group differences before the actual network analysis; (b) it visualizes individual connectivity matrices and individual network measures, which is crucial to detect potential outliers, a major confound in neuroimaging studies; (c) it carries out longitudinal graph theory analyses that provide an important insight into topological network changes over time; (d) it assesses modular structure using different algorithms and allows performing subnetwork analyses within the defined modules, which is important for studies testing hypotheses within a particular structural or functional brain network; (e) it provides utilities for multi-modal graph theory analysis by integrating information from different neuroimaging modalities, which is arguably the next challenge in imaging connectomics; for example, the user can compare structural (MRI) and functional (fMRI) data in BRAPH by defining the networks derived from both modalities with the same atlas. From the user point of view, BRAPH is the only fully vertically integrated software that allows carrying out all the steps of a graph theory analysis, from importing the neuroimaging data to saving the final results and the analysis parameters in a

2016-02282 2017-2020, and Birgitta och Sten Westerberg for additional financial support. We would also like to thank TÜBİTAK 2215 Graduate Programme for their support.

Competing interests: While commercial funding was obtained by the ADNI and PPMI initiatives, the authors have not directly received commercial funding. This does not alter our adherence to PLOS ONE policies on sharing data and materials.

single file. Importantly, this is not only practical but also increases the reliability and reproducibility of the results, which is an increasingly important issue within the research community. In addition, BRAPH offers a comprehensive manual, continuous release of new utilities, and a support forum, all of which can be accessed at http://www.braph.org/. Finally, BRAPH offers online videos that provide a step-by-step guide on how to perform graph theory analyses, allowing the users a simple and quick start for their brain connectivity studies.

Below we describe in detail the different options that BRAPH offers for graph theory analyses when it comes to building connectivity matrices, applying threshold strategies, performing weighted or binary network analyses and computing random networks. Our software has already been successfully applied in previous graph theory studies [27,28] but to further demonstrate its abilities, in this article we assess network topology on structural MRI data from patients with amnestic mild cognitive impairment (MCI) and AD, and on fMRI data from PD patients with MCI.

Materials and methods

Overview of BRAPH

BRAPH is a complete software package that allows carrying out all the steps of a graph theoretical analysis, visualize the results and generate high-quality publication-ready images. It can obtain undirected binary and weighted brain connectivity graphs starting from data acquired using various neuroimaging modalities, including MRI, fMRI, EEG, and positron emission tomography (PET). BRAPH can also assess the modular structure of the brain graph, employing various algorithms and extracting modules for further analysis. To test for significant differences between groups, BRAPH carries out non-parametric permutation tests and allows correcting the results for multiple comparisons using false discovery rate (FDR) [29]. It also provides options to normalize the network measures by random graphs as well as to carry out longitudinal graph theory analyses, the statistical significance of which is reported by non-parametric permutation tests.

As shown in Fig 1, the software consists of three independent layers connected by software interfaces: Graph, Data Structures and Graphical User Interfaces (GUIs). The Graph package includes the fundamental functions to perform a graph theory analysis and calculating the global and nodal measures. The Data Structures package provides the core functionalities of the software and allows defining the brain atlas, the cohort of subjects, and the type of graph analysis; importantly, all these functionalities can be accessed by command-line and can therefore be scripted by advanced users. Finally, the GUIs package provides a streamlined way to carry out graph theory analyses based on a series of GUIs for users without a computational background: (a) the *GUI Brain Atlas* allows selecting and editing the brain atlas; (b) the *GUI Cohort* allows defining the cohort of subjects by uploading the relevant data; (c) the *GUI Graph Analysis* allows building the connectivity matrices by selecting the type of graph (*weighted*, *binary*, see also Fig 2) and thresholding method (*threshold*, *density*) as well as calculating topological measures and visualizing the results. For the *GUI Cohort* and *GUI Graph Analysis*, four options can be selected (MRI, fMRI, PET, EEG) depending on the nature of the analysis. Fig 3 shows an overview of these different steps. Thanks to this three-layered structure, BRAPH can be easily expanded and customized to address any needs, e.g., by implementing new graph measures or new approaches for building brain graphs.

Defining the nodes

The first step of a graph theory analysis consists of defining the nodes, which generally correspond to the regions included in a brain atlas. This atlas should contain the names and labels

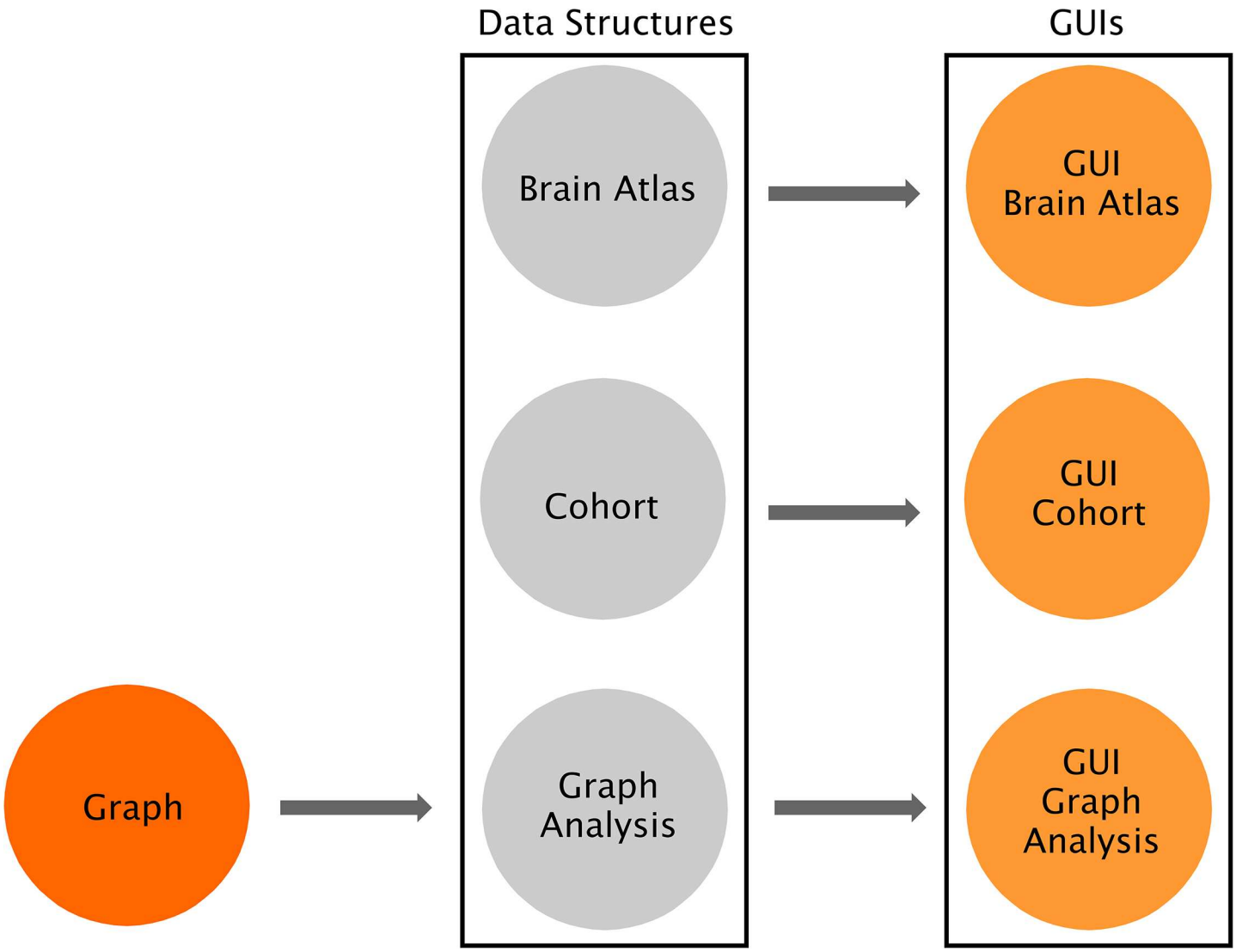

Fig 1. Overview of BRAPH software architecture. BRAPH consists of three layers, from left to right: *Graph*, *Data Structures* and *Graphical User Interfaces* (GUIs). These layers are connected by unidirectional software interfaces (arrows). *Graph* contains the functions to perform graph analyses. In *Data Structures*, *Brain Atlas* allows defining the nodes of the network, *Cohort* allows defining the subjects to be studied and dividing them into groups, and *Graph Analysis* permits building the connectivity matrices and calculating network measures; each of these is implemented in an object, whose functionalities can be called by command line. For each of these objects, a GUI is provided (i.e. *GUI Brain Atlas*, *GUI Cohort* and *GUI Graph Analysis*). Thanks to this architecture BRAPH can be very easily maintained, expanded and customized.

https://doi.org/10.1371/journal.pone.0178798.g001

of the brain regions as well as their spatial coordinates (x, y, z) in order to project them onto a 3D surface and create a visual representation of the brain graph. In the case of the analysis of structural networks (e.g. obtained from structural MRI data or T_1-weighted images), the nodes are usually defined using an anatomical parcellation scheme that divides the brain into regions using the brain sulci and gyri as anatomical landmarks. Examples of anatomical atlases are the automated anatomical labeling (AAL) [30], Desikan [31] or Destrieux [32] atlases. BRAPH already provides these atlases ready for upload on the *GUI Brain Atlas* interface. In the case of the analysis of functional networks (e.g. obtained from fMRI data), the atlas may be defined using an anatomical parcellation scheme, a meta-analysis, or a clustering-based method of spatially coherent and homogenous regions. Examples of functional atlases are the Dosenbach

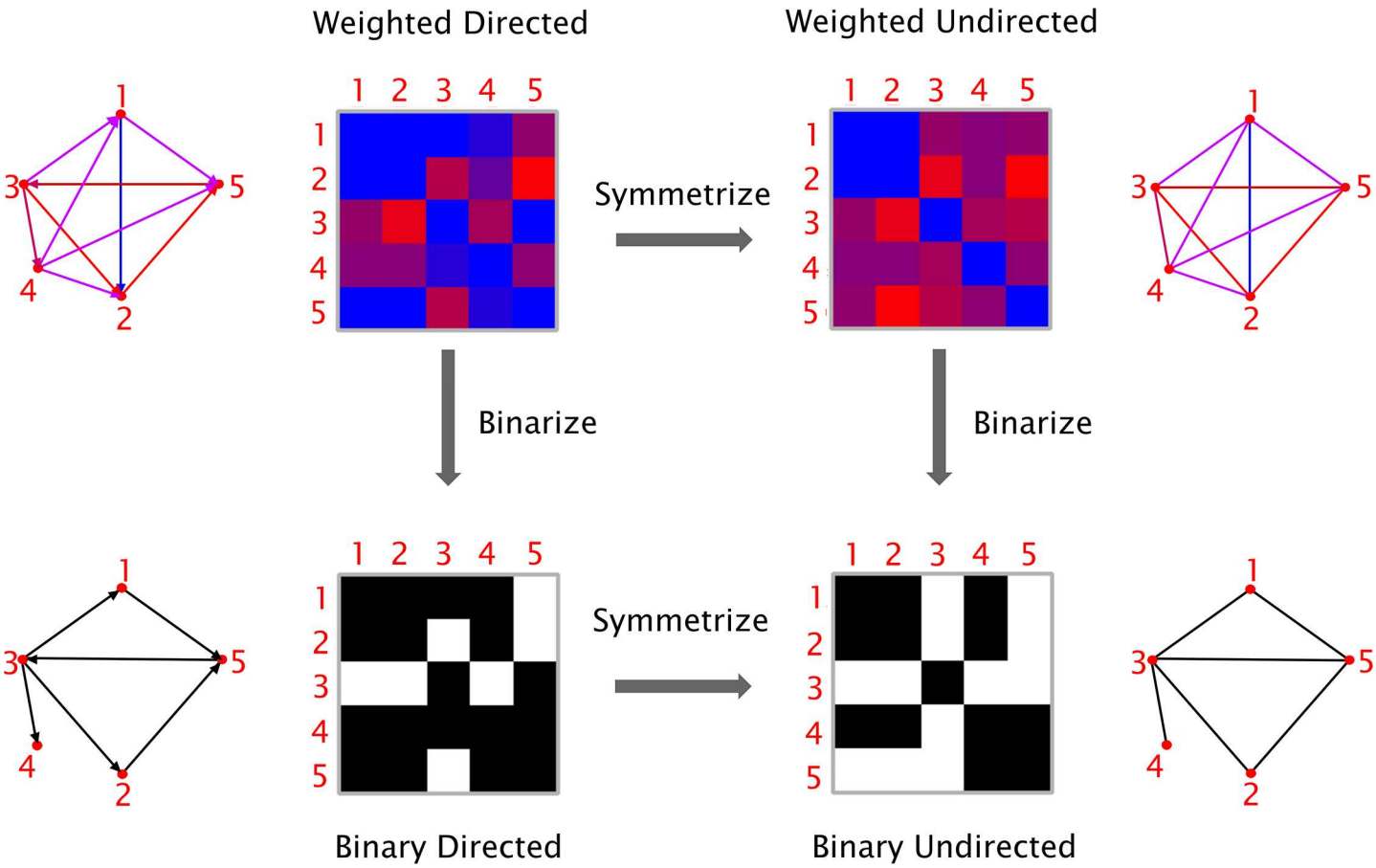

Fig 2. Types of graphs. Graphs can be classified based on their edge weights (*weighted* or *binary*) and directionality (*directed* or *undirected*). It is possible to transform a directed graph into an undirected one by symmetrization (i.e. by removing the information about the edge directions), and a weighted graph into a binary one by thresholding (i.e. by assigning a value of 1 to the edges above a given threshold and 0 to those below threshold).

https://doi.org/10.1371/journal.pone.0178798.g002

[33], the Power [34] and the Craddock [35] atlases, all of which are also provided by BRAPH. The user may also upload a different atlas from an external file (in.xml,.txt or.xls format) or create an entirely new one in the GUI. The resulting atlas can be saved as a.atlas file (see manual and website for an example of a.atlas file).

After the atlas has been created or uploaded into the software, the user should then upload the subject data into the *GUI Cohort* interface. This data may consist, for example, of cortical thickness, surface area or volume measures in structural MRI; regional time-series in resting-state fMRI; glucose metabolism or blood flow in PET and ASL; and electrophysiological signals in EEG or MEG. These regional values can be obtained using the Statistical Parametric Mapping (SPM; http://www.fil.ion.ucl.ac.uk/spm/), FMRI Software Library (FSL; https://fsl.fmrib.ox.ac.uk/fsl/fslwiki), FreeSurfer (https://surfer.nmr.mgh.harvard.edu/) or any other image preprocessing software. In addition, they may be corrected for the effects of nuisance variables such as age, gender or scanner site by means, for example, of linear regression (in this case the residual values should substitute the raw values in the network analysis) [36].

Defining the edges

Once the nodes of the network have been defined, the edges representing the relationship between them need to be computed. In BRAPH, the edges are calculated in *GUI Graph*

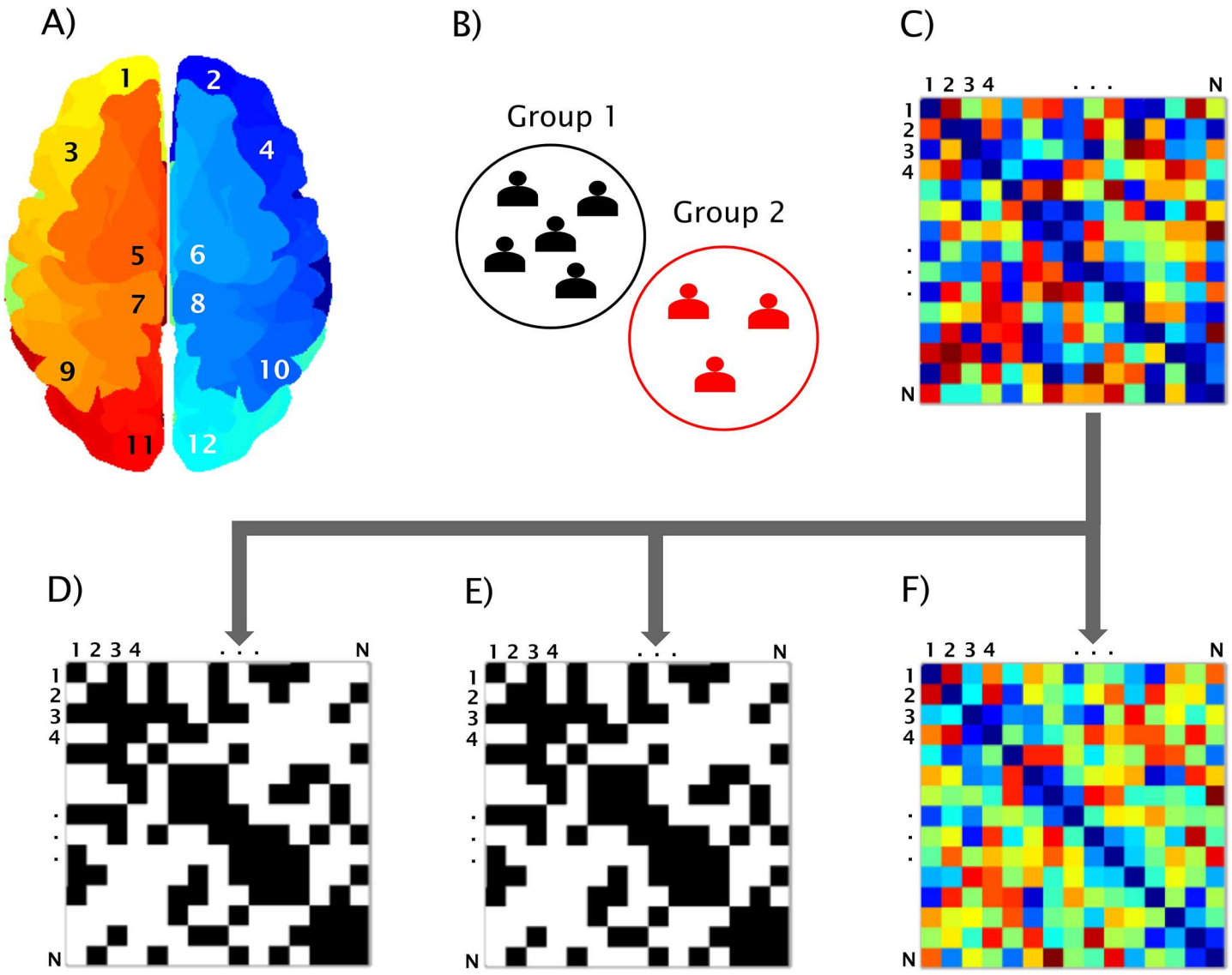

Fig 3. BRAPH workflow. Workflow for a graph theory analysis in BRAPH and relative graphical user interfaces (GUIs). A) The brain regions are defined in the *GUI Brain Atlas*. B) The data of the subjects are imported in the *GUI Cohort* and the user can define groups and edit their age, gender and other relevant data. C) The connectivity matrix is calculated in the *GUI Graph Analysis* after selecting the parameters defining the type of correlation, how to deal with negative correlation coefficients, and which type of graph to analyze: D) binary undirected graphs at a fixed density (*GUI Graph Analysis BUD*); E) binary undirected graphs at a fixed threshold (*GUI Graph Analysis BUT*); F) weighted undirected graphs (*GUI Graph Analysis WU*).

https://doi.org/10.1371/journal.pone.0178798.g003

Analysis as the statistical correlation between the values of all pairs of brain regions for an individual or for a group of subjects, depending on the neuroimaging technique. Different types of parametric and non-parametric correlations may be selected for this purpose: Pearson, Spearman, Kendall rank correlation coefficients, or (Pearson or Spearman) partial correlation coefficients. Note that all self-connections are eliminated from the analysis by setting the diagonal entries in the connectivity matrix to zero. In addition, the user can also choose whether to retain the negative correlation coefficients, substitute them with their absolute value, replace them by zero, or transform the values using an s-transform.

Network construction

To minimize the computation time, the graph measures can be calculated using optimized algorithms based on linear algebra. Therefore, a graph is more conveniently represented as a connectivity matrix, where the rows/columns denote the nodes and the matrix elements represent the edges between the nodes. Each row of the connectivity matrix represents the edges that are going out from a node; for example, row j represents the edges that are going out from node j. Each column of the matrix represents the nodes that arrive to a node; for example, column k represents the edges that are arriving to node k. Thus, the element (j, k) represents the edge that goes from node j to node k. The specific order of the nodes in the matrix does not affect the calculation of the graph theory measures, but only the graphical representation of the connectivity matrix. As illustrated in Fig 2, based on the nature of the edges' weight and directionality, four types of graphs can be defined. *Weighted directed* (WD) graphs have edges associated with a real number, indicating the strength of the connection, and are directed (i.e., node j can be connected to node k without node k being connected to node j). The edges in the *weighted undirected* (WU) graphs are associated with a real number indicating the strength of the connection and are undirected (i.e., if node j is connected to node k, then node k is also connected to node j), resulting in a symmetric connectivity matrix. *Binary directed* (BD) graphs have directed edges, which can either be 0 or 1, indicating the absence or presence of a connection. The edges in a *binary undirected* (BU) network can also be either 0 or 1 and they have no directionality. In order to transform a directed graph into an undirected graph, the connectivity matrix needs to be symmetrized. In BRAPH, the connectivity matrix can be symmetrized via command line by: (a) taking the sum between the matrix itself and its transpose; (b) taking the difference between the previous two; (c) comparing the matrix to its transpose and selecting either the smaller or the larger value for each entry. We remark that, even though the directed measures are not currently used in the analyses performed by BRAPH, they are already available in the *Graph* package and ready to be used in future versions of the software.

To transform a weighted graph into a binary one, BRAPH assigns a value of 1 to the edges above a given threshold and 0 to those below it. There are two ways of applying a threshold: (a) by selecting a correlation coefficient as the cut-off value below which all connections are excluded from the analysis (*binary undirected threshold* (BUT) interfaces); or (b) by fixing the fraction of edges (i.e., a specific density) that will be connected (*binary undirected density* (BUD) interfaces). The choice between these two options becomes significant when comparing different groups of subjects, as it may lead to different results; currently the density approach is more often employed in the literature, because it permits analyzing differences in network architecture while controlling for the different number of edges across individuals or groups. Additionally, BRAPH can be straightforwardly extended to include any alternative approach to determine the threshold, such as using a threshold-dependent cost function [37], maintaining the degree for each graph [38], keeping the ratio of strongest edges fixed [39], or using a heuristic approach based on the Dijkstra's algorithm [40]; all these approaches can be implemented by creating new objects analogous to MRIGraphAnalysisBUT or MRIGraphAnalysisBUD, and adapting the already existing methods in BRAPH.

For MRI or static PET data, a single connectivity matrix is calculated for each group of subjects; therefore, the graph theory measures reflect the group's properties. For fMRI data and other neuroimaging sequences that provide a measure of brain function over time, an individual connectivity matrix is calculated for each subject; therefore, the graph theory measures reflect the characteristics of each subject, which can then be averaged within a particular group.

Network analysis

BRAPH allows calculating both global and nodal network measures, on weighted or binary networks, using different thresholds or densities. To test for significant differences between groups (cross-sectional analysis) or two different points across time (longitudinal analysis), BRAPH performs non-parametric permutation tests, reporting one-tailed and two-tailed p-values based on 95% confidence intervals. The tests are performed by first randomly permuting the subjects from both groups and then calculating the differences in the graph measures between the new randomized groups. By repeating this procedure multiple (typically 1000 or 10000) times, a distribution of between-group differences is obtained. The p-values are then calculated as the fraction of the difference distribution values that exceeded the difference value between the actual groups. The same procedure is employed for the analysis of the longitudinal data with the difference that only the data corresponding to the same subject at different time points are permuted in order to prevent a group from containing the subject's data from two data points.

The network measures can also be compared with the corresponding measures calculated on random graphs with the same degree or weight distribution. These can be used, for example, to normalize weighted network measures. The needed random graphs are generated using the algorithms provided in the Brain Connectivity Toolbox [16].

Regarding nodal network measures, the permutation tests are carried out for each brain region, assessing simultaneously multiple null hypotheses, which consequently increases the risk of finding false positives. BRAPH deals with this issue by providing the adjusted p-values that should be considered to correct the results for multiple comparisons with false discovery rate (FDR) using the Benjamini-Hochberg procedure [29].

Graph theory measures

BRAPH can calculate several graph theory measures that assess the topology of the whole brain network as well as of its regions. Here, we explain briefly some of the most relevant ones; for a complete list with formulas and details, please refer to the BRAPH manual and website. The code we used to calculate the graph measures was adapted from the Brain Connectivity Toolbox (http://www.brain-connectivity-toolbox.net/) [16], which is regarded as the most important reference in the field since it provided the seminal groundwork for the use of graph theory by neuroimaging researchers.

The simplest, yet most fundamental, measure that can be assessed in a graph is the *degree*, which is the number of connections a node has with the rest of the network. The degree distribution in the brain follows an exponentially bound power law [41] meaning that similarly connected areas tend to communicate with each other [42]. In weighted graphs, BRAPH allows the user to calculate the nodal *strength* as well as nodal degree: the nodal strength is given by the sum of the weights of all connections linked to the node; and the nodal degree is the total number of the node's connections (thus assuming each edge has weight 1, making it analogous to the case of binary graphs).

Another important measure is the *shortest path length*, which is the shortest distance between two nodes. In a binary graph, distance is measured as the minimum number of edges that need to be crossed to go from one node to the other. In a weighted graph, the length of an edge is a function of its weight; typically, the edge length is inversely proportional to the edge weight because a high weight implies a stronger connection. The average of the shortest path lengths between one node and all other nodes is the *characteristic path length* [2]. One can also define two related measures of centrality: the *closeness centrality*, which is the inverse of the shortest path length, and the *betweenness centrality*, which is the fraction of all shortest paths

in the network that pass through a given node [16]. These and other measures can be used to assess whether a node is a brain hub [43], regulating most of the information flow within the network.

The closer the nodes are to each other, the shorter is the path length and the more efficient is the transfer of information between them. Therefore, one can define the *global efficiency* of a node as the inverse of the shortest path from that node to any other node in the network [44]. To assess the communication efficiency between a node and its immediate neighbors, the *local efficiency* can be calculated. Both global and local efficiency measures can be averaged over all nodes to describe global properties of the brain network [44].

The *clustering coefficient* is a measure that assesses the presence of cliques or clusters in a graph [2]. For each node, this can be calculated as the fraction of the node's neighbors that are also neighbors of each other. For the whole network, the nodal clustering coefficients of all nodes can be averaged into the mean clustering coefficient. A closely related measure to the clustering is the *transitivity*, which is defined as the ratio of paths that transverse two edges to the number of triangles. If a node is connected to another node, which in turn is connected to a third one, the transitivity reflects the probability that the first node is connected to the third.

The *small-worldness* is given by the ratio between the characteristic path length and mean clustering coefficient (normalized by the corresponding values calculated on random graphs) [2]; this is an important organizational property that describes an optimal network architecture. Compared to a random graph, a small-world network is characterized by similarly short paths but a significantly higher clustering coefficient.

A network can also be divided into separate communities corresponding to anatomical proximity or to a specific function shared by a group of nodes. The extent to which a network can be divided into these communities or modules can be calculated using the *modularity*, which maximizes the number of edges within communities and minimizes the number of edges between different communities [45]. The *within-module z-score* quantifies how well a node is connected with other nodes from the same module, while the *participation coefficient* assesses if a node has many connections with nodes from different modules. If a node has a high within-module degree, it is considered a provincial hub; if it has a high participation coefficient, it is considered a connector hub.

Subjects

To demonstrate the abilities of BRAPH, we performed structural and functional graph theory analyses in two separate studies. In the first study, we assessed the differences in global and nodal network topology in healthy controls, patients with amnestic MCI, and patients with AD (see Table 1) from the Alzheimer's Disease Neuroimaging Initiative (ADNI) database (adni.loni.usc.edu). The ADNI was launched in 2003 as a public–private partnership, led by Principal Investigator Michael W. Weiner, MD. The primary goal of ADNI has been to test whether serial MRI, PET, other biological markers, and clinical and neuropsychological assessment can be combined to measure the progression of MCI and early AD. All participants were scanned on a 1.5 Tesla MRI system using a sagittal 3D T_1-weighted MPRAGE sequence: repetition time (TR) = 9–13 ms; echo time (TE) = 3.0–4.1 ms; inversion time (IT) = 1000 ms; flip angle (FA) = 8°; voxel size = 1.1×1.1×1.2 mm^3.

In the second study, we carried out a graph theory analysis on the resting-state fMRI data of healthy controls, PD patients that were cognitively normal and PD patients with MCI (see Table 2) from the Parkinson's Progression Markers Initiative (PPMI) (2011) [46] (www.ppmi-info.org/data; accessed in November, 2015), an international, multicenter study launched in 2010 to identify PD progression biomarkers. PD patients were classified as having MCI

Table 1. Characteristics of the structural MRI sample.

	CTR (n = 210)	MCI (n = 377)	AD (n = 181)	F or $\chi 2$ (p value)
Age (y)	76.1(5.0)	74.5(7.5)	75.6 (7.0)	0.017
Sex (M/F)	110/100	243/134	97/84	0.005
Education (y)	16.0(2.9)	15.7(3.0)	14.8(3.2)	<0.001
MMSE	29.1(0.9)	27.0(1.8)	23.2(2.0)	<0.001

Means are followed by standard deviations. Differences in age, years of education, and MMSE scores were assessed using an analysis of variance (ANOVA). Differences in gender were assessed using a $\chi 2$ test. CTR, controls; MCI, mild cognitive impairment; AD, Alzheimer's disease; MMSE, mini-mental state examination.

https://doi.org/10.1371/journal.pone.0178798.t001

(PD-MCI) if they scored 1.5 standard deviations below the scaled mean scores on any two cognitive tests, following previously published procedures for PD-MCI diagnosis in the PPMI cohort [47]. Patients that did not fulfill criteria for MCI were classified as cognitively normal (PD-CN). All PD patients and controls were scanned on a 3 Tesla Siemens scanner (Erlangen, Germany). Resting-state functional images were acquired using an echo-planar imaging sequence (repetition time = 2400 ms; echo time = 25 ms; flip angle = 80°; matrix = 68×68; voxel size = 3.25×3.25×3.25 mm^3). The scan lasted 8 minutes and 29 seconds and included 210 volumes.

Each participating site in ADNI and PPMI received approval from an ethical standards committee before study initiation and obtained written informed consent from all participants.

Network construction and analysis

To assess structural network topology in controls, amnestic MCI patients, and AD patients from ADNI, the T_1-weighted images of these subjects were preprocessed using FreeSurfer (version 5.3), as published elsewhere [28]. The cortical thickness and subcortical volumes of 82 regions were extracted and included as nodes in the network analysis. The edges between these regions were computed as Pearson correlations, setting the negative correlations to zero, and the network analyses were carried out on the binary undirected graphs, while controlling for the number of connections, across a range of densities from 5% to 25%, in steps of 0.5%.

To assess functional network topology in PD-CN patients, PD-MCI patients and a group of elderly controls from PPMI, fMRI images were preprocessed using SPM8 (http://www.fil.ion.

Table 2. Characteristics of the fMRI sample.

	CTR (n = 15)	PD-CN (n = 69)	PD-MCI (n = 15)	CTR vs PD-CN (p value)	CTR vs PD-MCI (p value)	PD-CN vs PD-MCI (p value)
Age (y)	66.4(9.1)	61.0(10.4)	63.5(8.2)	0.066	0.372	0.378
Sex (M/F)	13/2	46/23	11/4	0.125	0.361	0.616
Education (y)	16.5(2.3)	15.3(2.9)	14.2(3.1)	0.112	0.024	0.204
UPDRS-III	-	18.2(9.1)	21.8(8.9)	-	-	0.161
HY stage	-	1.7(0.5)	1.8(0.4)	-	-	0.297
MoCA	27.9(1.6)	27.6(1.9)	24.0(3.7)	0.615	0.001	<0.001
Disease duration (y)	-	1.2(0.9)	2.4(1.5)	-	-	<0.001

Means are followed by standard deviations. Differences in age, years of education, and MoCA scores were assessed using Student's T test. Differences in gender were assessed using a $\chi 2$ test. CTR, controls; PD-CN, Parkinson's disease cognitively normal; PD-MCI, Parkinson's disease with mild cognitive impairment; UPDRS-III, Unified Parkinson's disease rating scale–Part III; HY stage, Hoehn and Yahr stage; MoCA, Montreal cognitive assessment scale.

https://doi.org/10.1371/journal.pone.0178798.t002

ucl.ac.uk/spm) using the following steps: removal of first five volumes, slice-timing correction, realignment, normalization to the Montreal Neurological Institute (MNI) template (voxel size 3×3×3 mm^3), temporal filtering (0.01–0.08 Hz), regression of white matter, cerebrospinal fluid signals and six head motion parameters. The regional time-series of the 200 brain regions included in the Craddock atlas [35] were extracted from each subject. To compute the relationship between these regions, we used Pearson correlations and performed the network analyses on the weighted undirected graphs.

In both studies, non-parametric permutation tests with 10000 permutations were carried out to assess differences between groups, which were considered significant for a two-tailed test of the null hypothesis at $p<0.05$. In addition, to adjust the nodal network results for multiple comparisons, an FDR procedure was applied to control for the number of regions that were tested at $q<0.05$.

Results

Structural network topology in amnestic MCI and AD

The structural correlation matrices and brain graphs of patients and controls can be found in Fig 4. All groups showed strong correlations between bilaterally homologous regions.

Regarding global network topology (Fig 5), we found increases in the characteristic path length and local efficiency in MCI and AD patients compared to controls at several network densities. The transitivity and modularity showed the most widespread topological changes: the transitivity was decreased and the modularity was increased in MCI and AD patients across almost all network densities compared to controls. Compared to MCI, AD patients showed increases in the characteristic path length at a few network densities and widespread changes in the transitivity and modularity.

Regarding regional network topology (Fig 6), the nodal degree showed significant increases in the left medial orbitofrontal, right insula, bilateral rostral anterior cingulate and posterior cingulate gyri in addition to decreases in the left middle temporal, right precentral and right inferior parietal gyri in AD patients compared to controls. When compared to MCI, AD patients also presented a higher nodal degree in the left rostral anterior cingulate and isthmus cingulate gyri.

We also compared the nodal local efficiency between groups. This measure showed significant increases in the left transverse temporal gyrus in MCI patients compared to controls. AD patients showed increases in the local efficiency in the bilateral temporal pole and left entorhinal cortex as well as decreases in several regions from the frontal (bilateral superior frontal, left pars triangularis, bilateral pars opercularis, right postcentral gyri), temporal (bilateral inferior temporal gyri, amygdala, hippocampus) and parietal (left inferior parietal, right precuneus) lobes. When the two patient groups were compared to each other, AD patients showed efficiency increases in the right rostral anterior cingulate compared to the MCI group.

Functional network topology in PD-MCI

The functional connectivity matrices of controls, PD-CN and PD-MCI patients can be found in Fig 7. The comparison of the weighted average degree showed that both PD-CN and PD-MCI patients presented a lower number of connections compared to controls (PD-MCI = 172.6; PD-CN = 175.2; controls = 183.7), which showed a trend towards significance in the comparison with PD-CN (p-value = 0.081) and was statistically significant in the comparison with PD-MCI (p-value = 0.027). Then, we performed a modularity analysis on the weighted graphs of each group to assess the presence of smaller communities of regions (modules). This analysis showed there were five modules in controls, PD-CN and PD-MCI patients, which

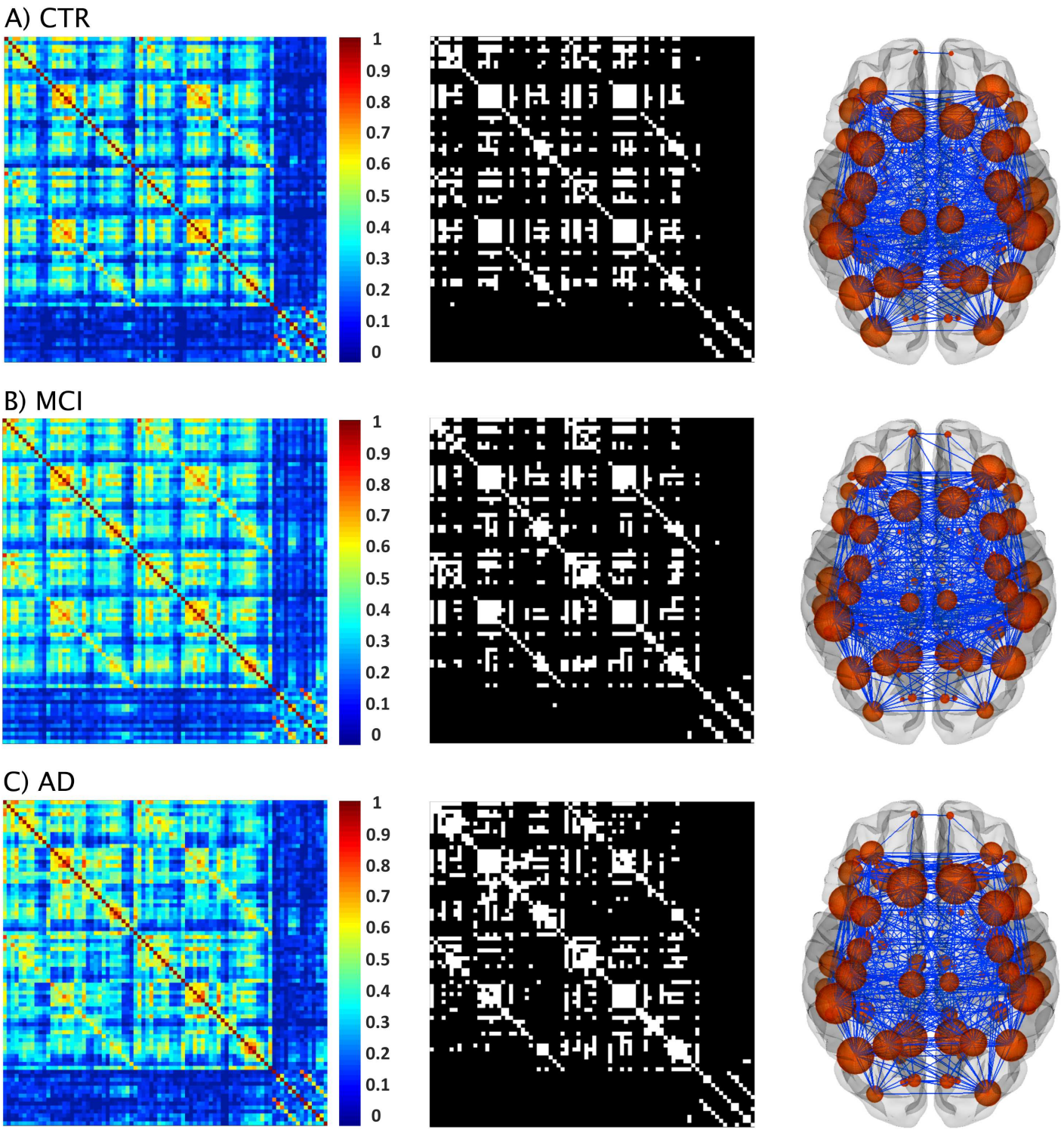

Fig 4. Structural brain networks in controls, MCI patients, and AD patients. From left to right: weighted correlation matrices of 82 regions, binary correlation matrices after fixing density at 15%, and corresponding brain graphs from A) controls (CTR), B) patients with amnestic mild cognitive impairment (MCI), and C) Alzheimer's disease (AD) patients.

https://doi.org/10.1371/journal.pone.0178798.g004

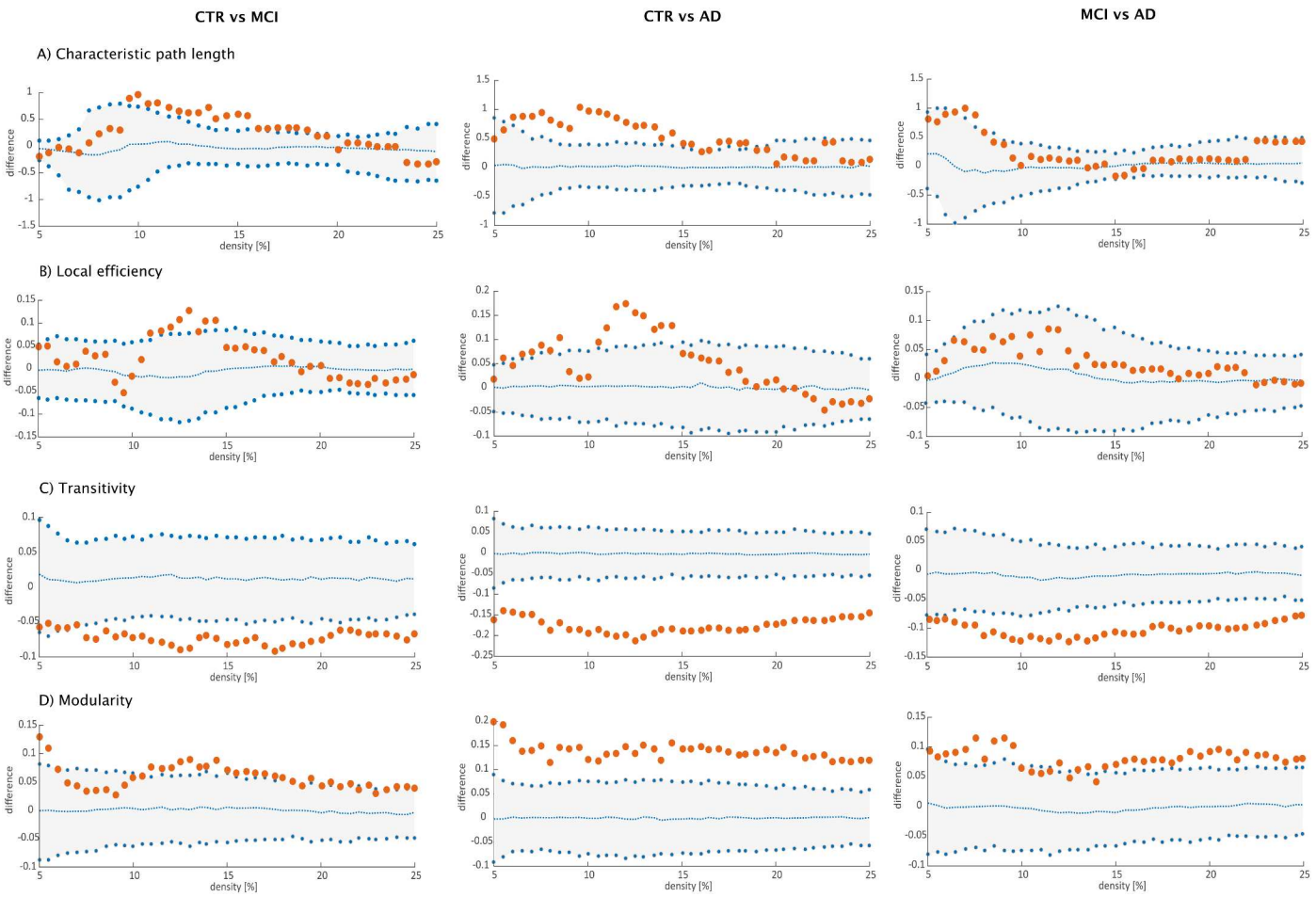

Fig 5. Differences between groups in global structural topology. Left: differences between controls (CTR) and Alzheimer's disease (AD) patients; middle: differences between controls (CTR) and patients with mild cognitive impairment (MCI); right: differences between patients with mild cognitive impairment (MCI) and Alzheimer's disease (AD) patients for A) characteristic path length, B) local efficiency, C) transitivity and D) modularity. The plots show the lower and upper bounds (blue circles) of the 95% Confidence Intervals (CI) (gray shade) as a function of density. The orange circles show the differences between groups and, when falling outside the CI, indicate that the difference was statistically significant at $p<0.05$. The blue dots in the middle with values around zero indicate the mean values of the difference in global network measures between the randomized groups after permutation tests.

https://doi.org/10.1371/journal.pone.0178798.g005

were quite similar in the three groups. Module I included medial frontal areas, the posterior cingulate and bilateral angular gyri, resembling the default-mode network. Module II comprised temporal and cerebellar areas. Module III included several middle, inferior frontal and parietal regions, similarly to the fronto-parietal network usually found in resting-state studies [5,6]. Module IV consisted of most of the visual cortex similarly to the previously reported visual network. Finally, Module V included mainly temporal and inferior frontal areas as well as the insula.

When we assessed the average degree of each module, we observed that PD-CN patients had a lower number of connections compared to controls in Module II, which included temporal and cerebellar areas (PD-CN = 49.02; controls = 51.89; p-value = 0.020), and Module V consisting of insular, temporal and inferior frontal regions (PD-CN = 28.39; controls = 28.93; p-value = 0.040). The regions within each of these modules did not show significant differences between controls and PD-CN patients after applying FDR corrections.

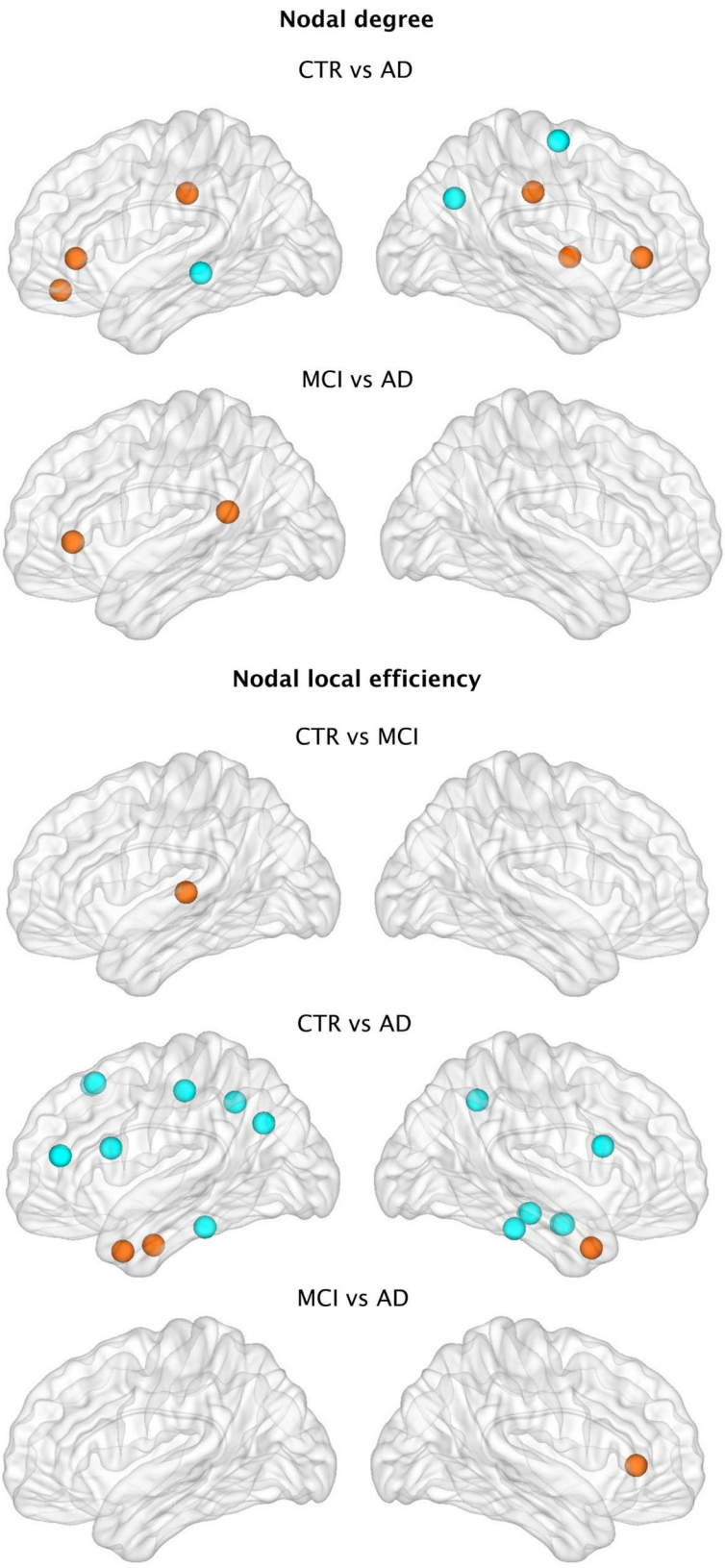

Fig 6. Differences between groups in nodal structural measures. Nodes showing significant differences between groups in the nodal degree and nodal local efficiency after FDR corrections. Orange indicates increases in nodal measures, while blue indicates decreases.

https://doi.org/10.1371/journal.pone.0178798.g006

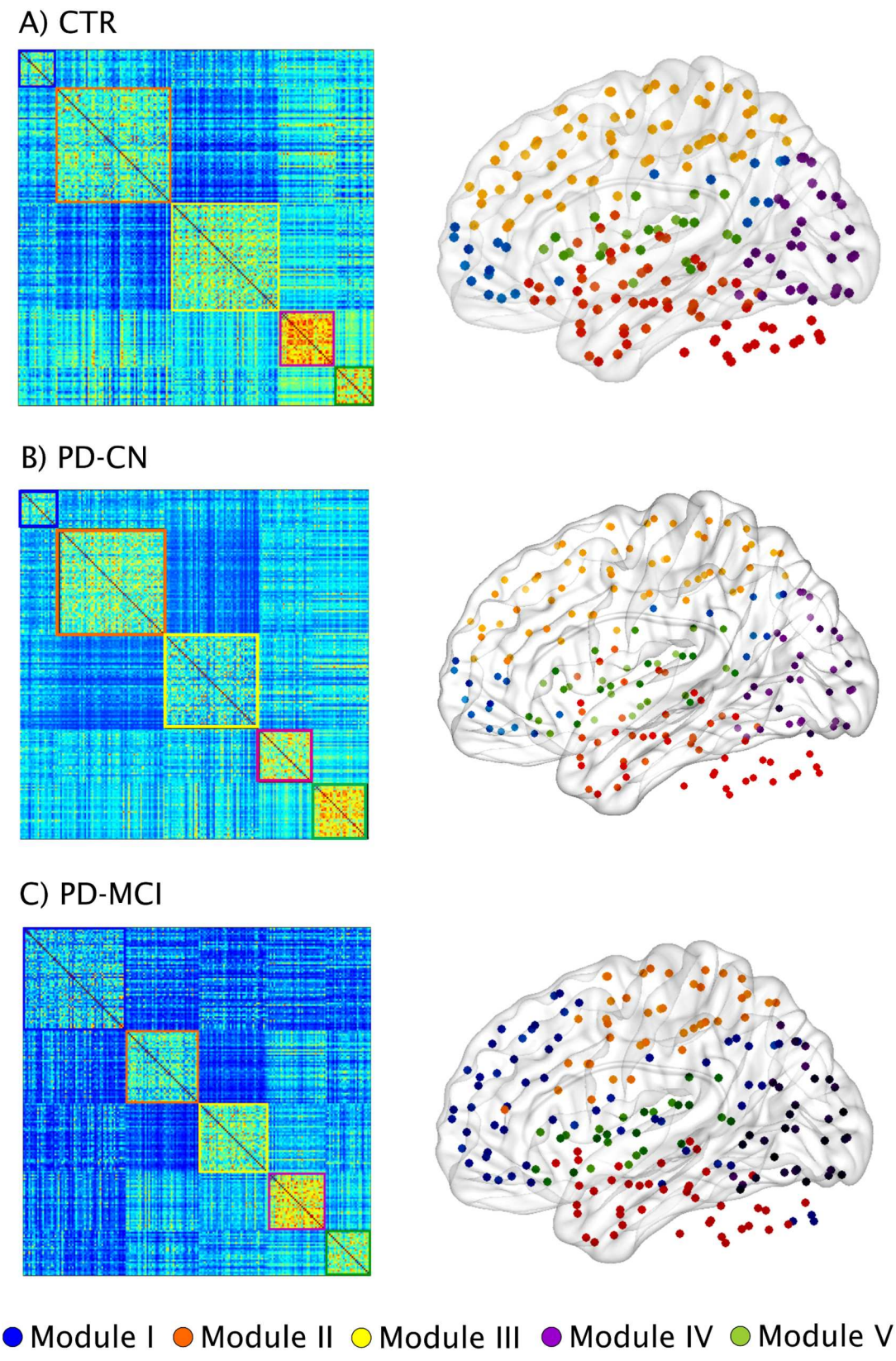

Fig 7. Functional brain networks and modules in controls and PD-MCI patients. Weighted connectivity matrices and modules in A) controls (CTR) and Parkinson's disease patients B) with normal cognition (PD-CN) and C) with mild cognitive impairment (PD-MCI). Five modules were identified in each group.

https://doi.org/10.1371/journal.pone.0178798.g007

We also found that, with respect to controls, PD-MCI patients had a lower number of connections in Module III comprising fronto-parietal areas (PD-MCI = 54.87; controls = 57.95; p-value = 0.002) and Module V involving insular, temporal and inferior frontal areas (PD-MCI = 28.37; controls = 28.93; p-value = 0.040). Within Module III, the regions showing a significantly lower degree in PD-MCI patients after FDR corrections were the bilateral superior frontal, bilateral superior parietal gyri, precuneus, left middle frontal gyrus, inferior frontal gyrus and left anterior cingulate (Fig 8A). Within Module V, the regions showing a significantly lower degree in PD-MCI patients after FDR corrections were the left insula, right frontal orbital gyrus and bilateral transverse temporal gyri (Fig 8B).

To assess whether the presence of different MCI subtypes influenced the results in the PD-MCI group, we compared the average degree and the nodal degree of Modules III and V between each subtype and controls. In this study, the PD-MCI group consisted of 9 patients with multiple-domain MCI and 6 patients with single-domain MCI (5 amnestic, 1 patient non-amnestic). These two subtypes showed lower average degree in Module III (multiple-domain MCI = 54.6; single-domain MCI = 55.3; controls = 58.0) and Module V (multiple-domain MCI = 28.4; single-domain MCI = 28.3; controls = 28.9) compared to the control group. All the regions within these modules showed a lower nodal degree in the two MCI subtypes compared to controls, except the right transverse temporal gyrus, which had a similar degree in controls and single-domain MCI patients (S1 Table).

Discussion

Graph theory has introduced new opportunities for understanding the brain as a complex system of interacting elements. Thanks to this framework, we have come to appreciate that the human brain relies on fundamental aspects of network organization such as a small-world architecture, modular structure and vulnerable hubs. These properties allow our brains to evolve, grow and adapt within an environment presenting increasing cognitive demands, and their disruption accounts for some of the key aspects underlying pathology in neurological diseases. In this report, we present BRAPH, the first object-oriented software for graph theory analysis intended for all researchers, regardless of their scientific background. As modern network science continues to develop at an increasing pace, it is important to have a software that allows modifying existent code in a structured manner so that past knowledge can be easily integrated with new topological analyses and graph theory measures. We are currently working on some of these developments with a particular focus on multimodal analyses and effective connectivity measures. Amongst BRAPH's strengths is the fact that it deals with all the aspects of graph theory analysis, by providing the user with extensive assistance, from the first basic steps such as defining the nodes and edges to producing the final publication-ready figures of the results as well as to archiving the results and relative analysis procedure in a dedicated file. To get an impression on BRAPH's abilities, below we discuss some of the results we obtained in two different studies in patients with amnestic MCI, AD and PD-MCI.

Large-scale structural networks in amnestic MCI and AD

AD is currently one of the most prevalent neurodegenerative disorders, with a significant impact on society and caregiver burden [48]. Although the devastating impact of this condition has pushed forward a large research effort towards a more accurate diagnosis, the underlying effects of AD on network topology remain poorly understood. There is increasing evidence suggesting that the pathological hallmarks of AD, consisting of amyloid plaques neurofibrillary tangles, could spread in the brain through synapses and neural connections. Hence, the application

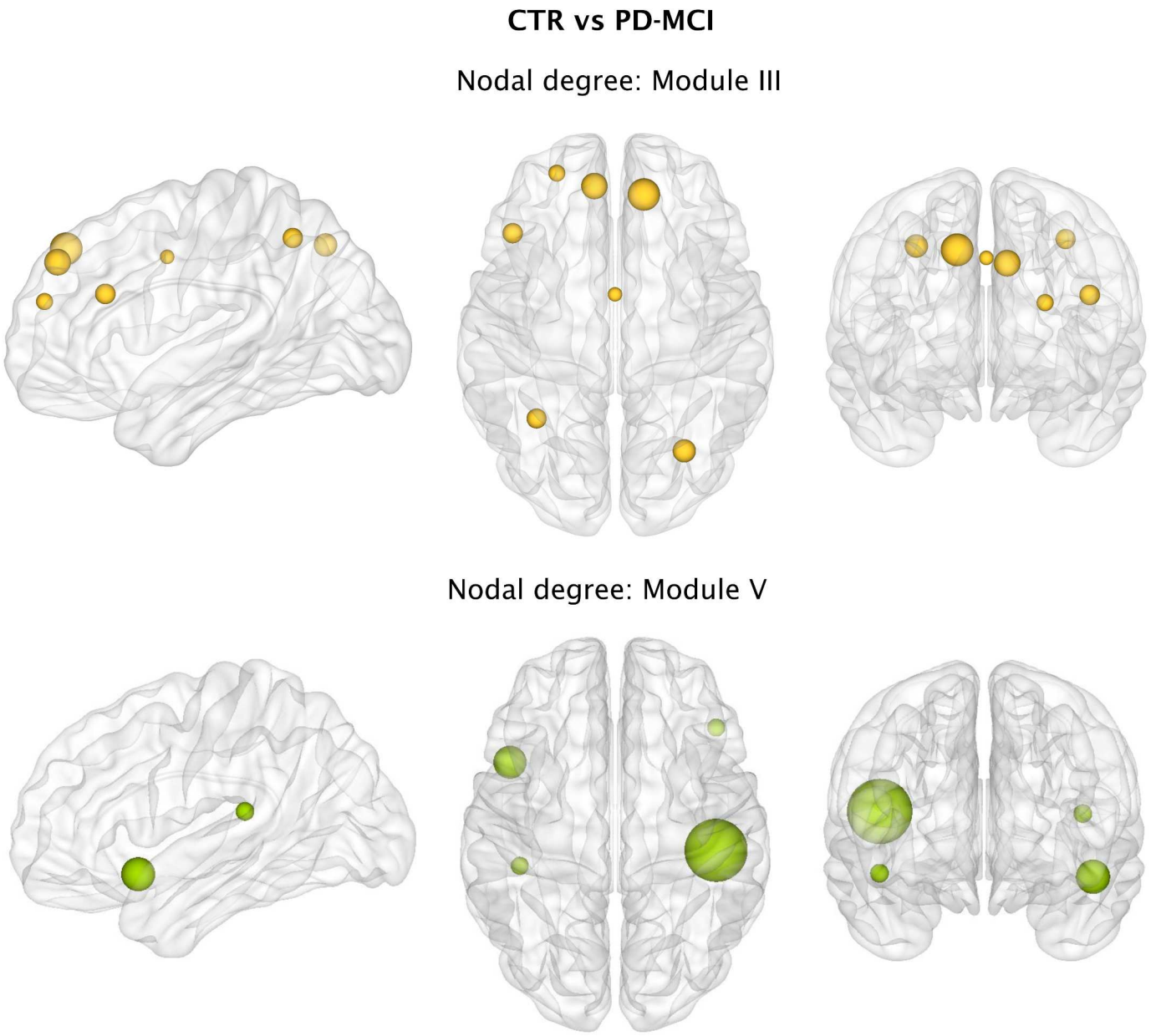

Fig 8. Differences between groups in the nodal functional degree. Significant decreases in the nodal degree of regions from Module III or fronto-parietal network in Parkinson's disease patients with mild cognitive impairment (PD-MCI) compared to controls (CTR) after FDR corrections.

https://doi.org/10.1371/journal.pone.0178798.g008

of graph theory to the study of brain connectivity could shed light on the mechanisms of disease propagation in AD.

In the current study, we found that AD patients presented an abnormal global network topology as reflected by increases in the path length, local efficiency and modularity, and by decreases of transitivity. These changes indicate that the regions of their networks communicated less efficiently with other brain regions and between different brain modules. In particular, the most widespread changes in network organization were observed for the transitivity and modularity. The decreases in transitivity found in AD suggest that the regions of their network were poorly connected to neighboring areas, whereas the increases in modularity

indicate that their modules had higher within-module connectivity and worse inter-module connectivity. Patients with amnestic MCI, who are potentially on the path to develop AD, also showed similar, albeit less extensive, network changes suggesting that amnesic MCI might be indeed an intermediate stage between healthy aging and dementia. These findings agree with the results obtained in previous studies [7, 28].

The assessment of the nodal degree in AD showed widespread changes in the number of connections of regions that belong to the default-mode network, including the medial orbitofrontal, the anterior cingulate and posterior cingulate gyri, compared to controls or patients with MCI. This network has been strongly associated with AD as its regions coincide with the areas showing amyloid deposition, gray matter atrophy and glucose hypometabolism in these patients [49]. Hence, the changes we found in this study may partially reflect pathological and metabolic abnormalities that usually occur in AD patients.

In contrast to the nodal degree, the nodal local efficiency showed alterations both in MCI and AD patients. Whereas in MCI patients, these changes were confined to a single region in the left temporal lobe, in AD patients the local efficiency was altered across several frontal, temporal and parietal areas, including the hippocampus and amygdala, which are involved in AD pathology [50]. The local efficiency reflects how efficient is the communication between a region and its neighboring areas. Decreases in this measure might indicate a loss of local connections, whereas increases could reflect a compensatory mechanism by which the number of connections between close brain areas increases to compensate for the loss of connections between distant brain areas.

Hence, altogether our findings indicate that graph theory is a useful method to assess abnormalities in brain connectivity and topology in the prodromal and clinical stages of AD.

Large-scale functional networks in PD

Cognitive impairment is one of the most important non-motor symptoms in PD that greatly affect quality of life. During the course of the disease, most PD patients develop impairment in one or more cognitive domains, for which they receive a diagnosis of MCI. The presence of MCI in PD is associated with an increased risk to progress to dementia [51]. Hence, there is a pressing need to identify the underlying mechanisms of MCI to prevent cognitive decline in PD patients. Using a weighted network approach in BRAPH, we found that PD-MCI patients presented a lower number of connections in the whole brain network compared to controls. This indicates that in general their regions were more disconnected. However, after identifying the modular structure and performing the same analysis within each module, we observed that these effects were mostly driven by a lower degree in the fronto-parietal network and in a network involving temporal and inferior frontal regions in the PD-MCI group. The regions that were most affected in these networks were the superior frontal gyri, superior parietal gyri, precuneus, transverse temporal gyri and insula. All of these regions have been previously shown to display reduced connectivity in PD [8]. In addition, they have also been identified as important brain hubs in previous graph theory studies [43]. Within the graph theory framework, the brain hubs are the most important and central regions of a network as they mediate numerous long-distance connections. This characteristic also suggests they might have higher metabolic costs and a greater vulnerability to oxidative stress [43]. In a previous study [52], it was shown that the pathological brain lesions are concentrated in hub regions of the connectome in several neurodegenerative disorders, including PD, in line with our findings. The analyses that were carried out in the separate single-domain and multiple-domain MCI groups showed that the previous regions had reduced connectivity in both subtypes, suggesting that our results in PD-MCI patients were not driven by a particular subgroup.

In addition to the results found in the PD-MCI group, we also found a reduced number of connections in PD-CN patients in two networks that consisted of temporo-cerebellar areas and temporo-frontal regions. Previous studies using fMRI have found abnormalities in these brain areas in patients with PD [8]. Moreover, the inferior temporal gyri and inferior frontal cortex are amongst the first cortical areas becoming affected by Lewy body pathology in autopsy cases with PD [53] suggesting that they might play a relevant role in the progression of the disease from brainstem structures to cortical brain areas. The fact that both PD-CN and PD-MCI patients showed abnormalities in the same network of inferior temporal and frontal areas provides support to this assumption and suggests that these regions are important to understand disconnectivity in PD regardless of cognitive status.

BRAPH features

The application of graph theory to the field of imaging connectomics is still in its early beginnings. There are several important challenges that need to be addressed such as whether the nodes and edges are an accurate description of the true underlying brain connectome in all its complexity of billions of neurons and synapses. Although we have limited knowledge on how to address this particular issue, there are several other challenges that can be addressed through the use of BRAPH. For instance, given that the true connectome is a sparse network, it is important to threshold the structural or functional edges, which typically consist of continuous association indices [54]. This thresholding can be carried out using different methods. On the one hand, a threshold can be applied so that only the connections that are below some significance level are included in the analysis. In this way, the weaker connections of the graph are eliminated and considered spurious. This approach will yield different numbers of connections across different individuals or groups. On the other hand, a threshold can be applied such that all networks have the same number of connections through a fixed value of density. In this way, only a percentage of edges are included in the analyses and the graph theory measures are independent of the number of edges [54]. In BRAPH, both thresholding options are available so that the user can easily compare them.

Another important challenge is the choice of a given value of threshold since there is currently no way to establish which is the best value. To solve this issue, BRAPH allows testing a hypothesis across different levels of significance or densities to determine the robustness of the results. Some authors consider choosing a range of thresholds an arbitrary process that produces values that are strongly dependent on this choice. For this reason, we also provide an option for weighted network analysis, which allows assessing both strong and weak connections present in a graph and is not dependent on a particular thresholding scheme.

Another challenge that is beginning to emerge in the scientific community is the realization that different node definitions can lead to different network findings. Currently BRAPH provides six anatomical and functional brain atlases that the user can apply within the same study to assess the consistency of the results against different parcellation schemes. In addition, a new brain atlas can be easily created or uploaded in BRAPH that adjusts to the user needs.

Finally, the last challenge that can be addressed through BRAPH is the normalization of graph theory measures by reference to random networks that have a random organization (with the same degree and/or weight distribution). BRAPH provides various options to perform this normalization.

Several aspects of BRAPH will be expanded in future releases. In particular, while currently BRAPH allows analyzing the complete fMRI time-series (static functional connectivity) by calculating statistical correlations or partial correlations between them since this is the most used method to analyze fMRI data, we are planning to include dynamic functional connectivity

analyses [23–26,55] in future versions of the software. Furthermore, we are also planning to allow the user to define the nodes using various data-driven methods, such as independent component analysis [55,56].

In conclusion, the study of the brain connectome is a growing field that will provide important insights into brain organization in health and disease. Amongst its numerous applications, there is the possibility it might help predicting the pathological spread of disease proteins in neurodegenerative disorders, which are becoming increasingly prevalent in the world's aging population. To address the increasing demands in this growing field we provide BRAPH, the first object-oriented software that will integrate new topological analyses and measures in a structured manner, allowing the users to be updated with the latest developments in graph theory. BRAPH can be found at https://www.braph.org with online videos, a comprehensive manual, a support forum and relevant links. It is free for all researchers and can be used in all operating systems.

Supporting information

S1 Table. Nodal degree for regions in Module III and V in PD-MCI subtypes and controls. Means are followed by standard deviations. CTR, controls; PD-CN, Parkinson's disease cognitively normal; PD-MCI, Parkinson's disease with mild cognitive impairment.
(DOCX)

Acknowledgments

Data used in preparation of this article were obtained from the Alzheimer's disease Neuroimaging Initiative (ADNI) database (adni.loni.ucla.edu). As such, the investigators within the ADNI contributed to the design and implementation of ADNI and/or provided data but did not participate in analysis or writing of this report. A complete listing of ADNI investigators can be found at: https://adni.loni.usc.edu/wp-content/uploads/how_to_apply/ADNI_Acknowledgment_List.pdf.

Author Contributions

Conceptualization: JBP EW GV.

Data curation: MM EK JBP.

Formal analysis: MM EK JBP.

Funding acquisition: JBP EW GV.

Investigation: MM EK JBP EW GV.

Methodology: MM EK JBP EW GV.

Project administration: GV.

Resources: JBP EW.

Software: MM EK GV.

Supervision: JBP EW GV.

Validation: MM EK JBP EW GV.

Visualization: MM EK JBP GV.

Writing – original draft: MM EK JBP.

Writing – review & editing: MM EK JBP EW GV.

References

1. Sporns O. The human connectome: origins and challenges. Neuroimage 2013; 80: 53–61. https://doi.org/10.1016/j.neuroimage.2013.03.023 PMID: 23528922
2. Watts DJ, Strogatz SH. Collective dynamics of 'small-world' networks. Nature 1998; 393: 440–442. https://doi.org/10.1038/30918 PMID: 9623998
3. Hagmann P, Cammoun L, Gigandet X, Meuli R, Honey CJ, Wedeen VJ, et al. Mapping the structural core of human cerebral cortex. PLoS Biol 2008; 6: e159. https://doi.org/10.1371/journal.pbio.0060159 PMID: 18597554
4. Meunier D, Stamatakis EA, Tyler LK. Age-related functional reorganization, structural changes, and preserved cognition. Neurobiol Aging 2014; 35: 42–54. https://doi.org/10.1016/j.neurobiolaging.2013.07.003 PMID: 23942392
5. Damoiseaux JS, Rombouts SA, Barkhof F, Scheltens P, Stam CJ, Smith SM, et al. Consistent resting-state networks across healthy subjects. Proc Natl Acad Sci U S A 2006; 103: 13848–13853. https://doi.org/10.1073/pnas.0601417103 PMID: 16945915
6. van den Heuvel MP, Hulshoff Pol HE. Exploring the brain network: a review on resting-state fMRI functional connectivity. Eur Neuropsychopharmacol 2010; 20: 519–534. https://doi.org/10.1016/j.euroneuro.2010.03.008 PMID: 20471808
7. Tijms BM, Wink AM, de Haan W, van der Flier WM, Stam CJ, Scheltens P, et al. Alzheimer's disease: connecting findings from graph theoretical studies of brain networks. Neurobiol Aging 2013; 34: 2023–2036. https://doi.org/10.1016/j.neurobiolaging.2013.02.020 PMID: 23541878
8. Baggio HC, Segura B, Junque C. Resting-state functional brain networks in Parkinson's disease. CNS Neurosci Ther 2015; 21: 793–801. https://doi.org/10.1111/cns.12417 PMID: 26224057
9. Liao W, Zhang Z, Pan Z, Mantini D, Ding D, Duan X, et al. Altered functional connectivity and small-world in mesial temporal lobe epilepsy. PloS ONE 2010, 5, e8525. https://doi.org/10.1371/journal.pone.0008525 PMID: 20072616
10. Zhang Z, Liao W, Chen H, Mantini D, Ding JR, Xu Q, et al. Altered functional–structural coupling of large-scale brain networks in idiopathic generalized epilepsy. Brain 2011, 134, 2912–2928. https://doi.org/10.1093/brain/awr223 PMID: 21975588
11. Ji GJ, Yu Y, Miao HH, Wang ZJ, Tang YL, Liao W. Decreased network efficiency in benign epilepsy with centrotemporal spikes. Radiology 2016, 160422.
12. Liu Y, Liang M, Zhou Y, He Y, Hao Y, Song M, et al. Disrupted small-world networks in schizophrenia. Brain 2008, 131, 945–961. https://doi.org/10.1093/brain/awn018 PMID: 18299296
13. Lynall ME, Bassett DS, Kerwin R, McKenna PJ, Kitzbichler M, Muller U, et al. Functional connectivity and brain networks in schizophrenia. Journal of Neuroscience 2010, 30, 9477–9487. https://doi.org/10.1523/JNEUROSCI.0333-10.2010 PMID: 20631176
14. Shu N, Liu Y, Li K, Duan Y, Wang J, Yu C, et al. Diffusion tensor tractography reveals disrupted topological efficiency in white matter structural networks in multiple sclerosis. Cerebral Cortex 2011, 21, 2565–2577. https://doi.org/10.1093/cercor/bhr039 PMID: 21467209
15. Barttfeld P, Wicker B, Cukier S, Navarta S, Lew S, Leiguarda R, et al. State-dependent changes of connectivity patterns and functional brain network topology in autism spectrum disorder. Neuropsychologia 2012, 50, 3653–3662. https://doi.org/10.1016/j.neuropsychologia.2012.09.047 PMID: 23044278
16. Rubinov M, Sporns O. Complex network measures of brain connectivity: uses and interpretations. Neuroimage 2010; 52: 1059–1069. https://doi.org/10.1016/j.neuroimage.2009.10.003 PMID: 19819337
17. He B, Dai Y, Astolfi L, Babiloni F, Yuan H, Yang L. eConnectome: A MATLAB toolbox for mapping and imaging of brain functional connectivity. J Neurosci Methods 2011; 195: 261–269. https://doi.org/10.1016/j.jneumeth.2010.11.015 PMID: 21130115
18. Hosseini SM, Hoeft F, Kesler SR. GAT: a graph-theoretical analysis toolbox for analyzing between-group differences in large-scale structural and functional brain networks. PLoS One 2012; 7: e40709. https://doi.org/10.1371/journal.pone.0040709 PMID: 22808240
19. Whitfield-Gabrieli S, Nieto-Castanon A. Conn: a functional connectivity toolbox for correlated and anticorrelated brain networks. Brain Connect 2012; 2: 125–141. https://doi.org/10.1089/brain.2012.0073 PMID: 22642651

20. Xia M, Wang J, He Y. BrainNet Viewer: a network visualization tool for human brain connectomics. PLoS One 2013; 8: e68910. https://doi.org/10.1371/journal.pone.0068910 PMID: 23861951
21. Kruschwitz JD, List D, Waller L, Rubinov M, Walter H. GraphVar: a user-friendly toolbox for comprehensive graph analyses of functional brain connectivity. J Neurosci Methods 2015; 245: 107–115. https://doi.org/10.1016/j.jneumeth.2015.02.021 PMID: 25725332
22. Wang J, Wang X, Xia M, Liao X, Evans A, He Y. GRETNA: a graph theoretical network analysis toolbox for imaging connectomics. Front Hum Neurosci 2015; 9: 386. https://doi.org/10.3389/fnhum.2015.00386 PMID: 26175682
23. Calhoun VD, Miller R, Pearlson G, Adali T. The chronnectome: time-varying connectivity networks as the next frontier in fMRI data discovery. Neuron 2014, 84, 262–274. https://doi.org/10.1016/j.neuron.2014.10.015 PMID: 25374354
24. Liao W, Zhang Z, Mantini D, Xu Q, Ji GJ, Zhang H, et al. Dynamical intrinsic functional architecture of the brain during absence seizures. Brain Structure Function 2014, 219, 2001–2015. https://doi.org/10.1007/s00429-013-0619-2 PMID: 23913255
25. Liao W, Wu GR, Xu Q, Ji GJ, Zhang Z, Zang YF, et al. DynamicBC: a MATLAB toolbox for dynamic brain connectome analysis. Brain Connectivity 2014, 4, 780–790. https://doi.org/10.1089/brain.2014.0253 PMID: 25083734
26. Cui J, Xu L, Bressler SL, Ding M, Liang H. BSMART: a Matlab/C toolbox for analysis of multichannel neural time series. Neural Networks 2008, 21, 1094–1104. https://doi.org/10.1016/j.neunet.2008.05.007 PMID: 18599267
27. Pereira JB, Aarsland D, Ginestet CE, Lebedev AV, Wahlund LO, Simmons A, et al. Aberrant cerebral network topology and mild cognitive impairment in early Parkinson's disease. Hum Brain Mapp 2015; 36: 2980–2995. https://doi.org/10.1002/hbm.22822 PMID: 25950288
28. Pereira JB, Mijalkov M, Kakaei E, Mecocci P, Vellas B, Tsolaki M, et al. Disrupted Network Topology in Patients with Stable and Progressive Mild Cognitive Impairment and Alzheimer's Disease. Cereb Cortex 2016; 26: 3476–3493. https://doi.org/10.1093/cercor/bhw128 PMID: 27178195
29. Benjamini Y, Hochberg Y. Controlling the false discovery rate: a practical and powerful approach to multiple testing. J Royal Stat Soc. Series B (Methodological) 1995; 289–300.
30. Tzourio-Mazoyer N, Landeau B, Papathanassiou D, Crivello F, Etard O, Delcroix N, et al. Automated anatomical labeling of activations in SPM using a macroscopic anatomical parcellation of the MNI MRI single-subject brain. Neuroimage 2002; 15: 273–289. https://doi.org/10.1006/nimg.2001.0978 PMID: 11771995
31. Desikan RS, Segonne F, Fischl B, Quinn BT, Dickerson BC, Blacker D, et al. An automated labeling system for subdividing the human cerebral cortex on MRI scans into gyral based regions of interest. Neuroimage 2006; 31: 968–980. https://doi.org/10.1016/j.neuroimage.2006.01.021 PMID: 16530430
32. Destrieux C, Fischl B, Dale A, Halgren E. Automatic parcellation of human cortical gyri and sulci using standard anatomical nomenclature. Neuroimage 2010; 53: 1–15. https://doi.org/10.1016/j.neuroimage.2010.06.010 PMID: 20547229
33. Dosenbach NU, Visscher KM, Palmer ED, Miezin FM, Wenger KK, Kang HC, et al. A core system for the implementation of task sets. Neuron 2006; 50: 799–812. https://doi.org/10.1016/j.neuron.2006.04.031 PMID: 16731517
34. Power JD, Cohen AL, Nelson SM, Wig GS, Barnes KA, Church JA, et al. Functional network organization of the human brain. Neuron 2011; 72: 665–678. https://doi.org/10.1016/j.neuron.2011.09.006 PMID: 22099467
35. Craddock RC, James GA, Holtzheimer PE, 3rd, Hu XP, Mayberg HS. A whole brain fMRI atlas generated via spatially constrained spectral clustering. Hum Brain Mapp 2012; 33: 1914–1928. https://doi.org/10.1002/hbm.21333 PMID: 21769991
36. Voevodskaya O, Simmons A, Nordenskjold R, Kullberg J, Ahlstrom H, Lind L, et al. The effects of intracranial volume adjustment approaches on multiple regional MRI volumes in healthy aging and Alzheimer's disease. Front Aging Neurosci 2014; 6: 264. https://doi.org/10.3389/fnagi.2014.00264 PMID: 25339897
37. Bassett DS, Bullmore E, Verchinski BA, Mattay VS, Weinberger DR, Meyer-Lindenberg A. Hierarchical organization of human cortical networks in health and schizophrenia. J Neurosci 2008, 28, 9239–9248. https://doi.org/10.1523/JNEUROSCI.1929-08.2008 PMID: 18784304
38. Stam CJ, Jones BF, Nolte G, Breakspear M, Scheltens P. Small-world networks and functional connectivity in Alzheimer's disease. Cerebral cortex 2007, 17, 92–99. https://doi.org/10.1093/cercor/bhj127 PMID: 16452642

39. Rubinov M, Knock SA, Stam CJ, Micheloyannis S, Harris AW, Williams LM, et al. Small-world properties of nonlinear brain activity in schizophrenia. Hum Brain Mapp 2009, 30, 403–416. https://doi.org/10.1002/hbm.20517 PMID: 18072237

40. Dimitriadis SI, Laskaris NA, Tsirka V, Vourkas M, Micheloyannis S, Fotopoulos S. Tracking brain dynamics via time-dependent network analysis. J Neurosci Methods 2010, 193, 145–155. https://doi.org/10.1016/j.jneumeth.2010.08.027 PMID: 20817039

41. Achard S, Salvador R, Whitcher B, Suckling J, Bullmore E. A resilient, low-frequency, small-world human brain functional network with highly connected association cortical hubs. J Neurosci 2006; 26: 63–72. https://doi.org/10.1523/JNEUROSCI.3874-05.2006 PMID: 16399673

42. Barabási AL. Network science. Cambridge University Press, 2016.

43. van den Heuvel MP, Sporns O. Network hubs in the human brain. Trends Cogn Sci 2013; 17: 683–696. https://doi.org/10.1016/j.tics.2013.09.012 PMID: 24231140

44. Latora V, Marchiori M. Efficient behavior of small-world networks. Phys Rev Lett 2001; 87: 198701. https://doi.org/10.1103/PhysRevLett.87.198701 PMID: 11690461

45. Girvan M, Newman ME. Community structure in social and biological networks. Proc Natl Acad Sci U S A 2002; 99: 7821–7826. https://doi.org/10.1073/pnas.122653799 PMID: 12060727

46. Parkinson Progression Marker Initiative. The Parkinson Progression Marker Initiative (PPMI). Prog Neurobiol 2011; 95: 629–635. https://doi.org/10.1016/j.pneurobio.2011.09.005 PMID: 21930184

47. Weintraub D, Simuni T, Caspell-Garcia C, Coffey C, Lasch S, Siderowf A, et al. Cognitive performance and neuropsychiatric symptoms in early, untreated Parkinson's disease. Mov Disord 2015; 30: 919–927. https://doi.org/10.1002/mds.26170 PMID: 25737166

48. Winblad B, Amouyel P, Andrieu S, Ballard C, Brayne C, Brodaty H et al. Defeating Alzheimer's disease and other dementias: a priority for European science and society. Lancet Neurol 2016; 15: 455–532. https://doi.org/10.1016/S1474-4422(16)00062-4 PMID: 26987701

49. Buckner RL, Snyder AZ, Shannon BJ, LaRossa G, Sachs R, Fotenos AF, et al. Molecular, structural, and functional characterization of Alzheimer's disease: evidence for a relationship between default activity, amyloid, and memory. J Neurosci 2005; 25: 7709–7717. https://doi.org/10.1523/JNEUROSCI.2177-05.2005 PMID: 16120771

50. Braak H, Braak E. Neuropathological stageing of Alzheimer-related changes. Acta Neuropathol 1991; 82: 239–259. PMID: 1759558

51. Svenningsson P, Westman E, Ballard C, Aarsland D. Cognitive impairment in patients with Parkinson's disease: diagnosis, biomarkers, and treatment. Lancet Neurol 2012; 11: 697–707. https://doi.org/10.1016/S1474-4422(12)70152-7 PMID: 22814541

52. Crossley NA, Mechelli A, Scott J, Carletti F, Fox PT, McGuire P, et al. The hubs of the human connectome are generally implicated in the anatomy of brain disorders. Brain 2014; 137: 2382–2395. https://doi.org/10.1093/brain/awu132 PMID: 25057133

53. Braak H, Del Tredici K, Rüb U, de Vos RA, Steur EN, Braak E. Staging of brain pathology related to sporadic Parkinson's disease. Neurobiology of aging. 2003 Apr 30; 24(2):197–211. PMID: 12498954

54. Fornito A, Zalesky A, Breakspear M. Graph analysis of the human connectome: promise, progress, and pitfalls. Neuroimage 2013; 80: 426–444. https://doi.org/10.1016/j.neuroimage.2013.04.087 PMID: 23643999

55. Yu Q, Erhardt EB, Sui J, Du Y, He H, Hjelm D, et al. Assessing dynamic brain graphs of time-varying connectivity in fMRI data: Application to healthy controls and patients with schizophrenia. Neuroimage 2015, 107, 345–355. https://doi.org/10.1016/j.neuroimage.2014.12.020 PMID: 25514514

56. Smith SM, Miller KL, Salimi-Khorshidi G, Webster M, Beckmann CF, Nichols TE, et al. Network modelling methods for FMRI. Neuroimage 201154, 875–891.